Simple approach to two-proton emission

D. S. Delion,[1,2,3] R. J. Liotta,[4] and R. Wyss[4]

[1] *"Horia Hulubei" National Institute of Physics and Nuclear Engineering, 407 Atomiştilor, RO-077125 Bucharest-Măgurele, România*

[2] *Academy of Romanian Scientists, 54 Splaiul Independenţei, RO-050085 Bucharest, România*

[3] *Bioterra University, 81 Gârlei, RO-013724 Bucharest, România*

[4] *KTH, Alba Nova University Center, SE-10691 Stockholm, Sweden*

(Received 1 June 2012; revised manuscript received 19 February 2013; published 28 March 2013)

The two-proton decay process is studied by using a simple approach within the framework of scattering theory. We assume that the decaying nucleus is in a pairing state and, therefore, the two-particle wave function on the nuclear surface corresponds to the two protons moving in time-reversed states. This allows us to sustain a simplified version of the decay where the protons are simultaneously emitted with the same energies. We thus obtain a coupled system of radial equations with outgoing boundary conditions. We use similar proton-proton interactions to solve BCS equations and to describe external two-proton dynamics. A strong dependence of the pairing gap and decay width upon the proton-proton interaction strength is revealed. The experimental half-lives of ^{45}Fe and ^{48}Ni are reproduced by using a realistic proton-proton interaction.

DOI: 10.1103/PhysRevC.87.034328 PACS number(s): 21.10.Tg, 23.50.+z, 25.70.Ef

I. INTRODUCTION

The radioactive process in which two protons are emitted is a very exotic mode of decay that is energetically possible in some nuclei only. In the earlier sixties Goldansky proposed two extreme mechanisms in which the particles are emitted, either simultaneouly or sequentially [1]. Due to different Coulomb barriers the penetrability in the two cases leads to decay widths differing from each other by several orders of magnitude. A systematic theoretical analysis of the processes involving the inherent three-body problem was performed for the first time in Ref. [2]. The interest in this subject has increased in recent years due to experimental advances that made possible the measurement of this rare event. The theoretical description of the decays was performed by using few-body formalisms [3–5] as well as R-matrix approaches [6,7]. Even techniques based on the Feshbach reaction theory and the continuum shell model were applied [8,9]. Still the old question of whether the two protons decay as a single cluster or whether they decay independently of each other remains. The one-proton decay systematics reveals simple two-body features depending on the Coulomb and centrifugal parameters [10]. The systematic analysis of decay processes indicates that the two-proton emission has a three-body character, between the diproton and pure sequential decay [11]. The exact three-body treatment in terms of hyperspherical coordinates or by using the continuum shell model is rather involved. We will consider that the two protons are emitted from a correlated pairing state. It is important to point out that the pairing interaction induces a clustering of the two protons. This is a fundamental property in α emission, because it explains the clustering of the four nucleons that eventually constitutes the α particle [12]. We use this property below by assuming that near the nuclear surface the two protons lie near each other.

In Sec. II we give the necessary theoretical background, in Sec. III we apply it to compute the two-proton decay width, and in the Sec. IV we draw conclusions.

II. THEORETICAL BACKGROUND

We start by pointing out that in medium nuclei, where we perform the calculations, the mass of the daughter nucleus is much larger than the mass carried by the decaying protons. We therefore neglect recoil effects. We consider that the parent and the daughter nuclei are spherical. The parent ground state (gs) $|P\rangle$ can be expanded in terms of the daughter gs $|D\rangle$ as

$$|P\rangle = \sum_{\epsilon lj} X_{\epsilon lj}[a^\dagger_{\epsilon lj}a^\dagger_{\epsilon lj}]_0|D\rangle, \tag{2.1}$$

where the operator $a^\dagger_{\epsilon lj}$ creates a single particle (sp) proton eigenstate of the mean field potential. In r representation it is

$$a^\dagger_{\epsilon ljm} \to \psi_{\epsilon ljm}(\mathbf{r},\mathbf{s}) = \frac{f_{\epsilon lj}(r)}{r}\left[i^l Y_l(\hat{r})\otimes\chi_{\frac{1}{2}}(\mathbf{s})\right]_{jm}, \tag{2.2}$$

where $f_{\epsilon lj}(r)$ is the radial wave function and the rest of the notation is standard. We assume that the states with positive energy are sp resonances. They are normalized to unity inside the Coulomb barrier and at large distances behave like outgoing Coulomb waves [13]:

$$f_{\epsilon lj}(r) \underset{r\to\infty}{\longrightarrow} M_{\epsilon lj}H^{(+)}_l(r) \equiv M_{\epsilon lj}[G_l(r) + iF_l(r)], \tag{2.3}$$

where $M_{\epsilon lj}$ defines the one-proton scattering amplitude.

In our calculations we consider that the two emitted protons are initially paired. Thus, the expansion coefficients,

$$X_{\epsilon lj} = \frac{1}{2}{}_P\langle \mathrm{BCS}|[a^\dagger_{\epsilon lj}\otimes a^\dagger_{\epsilon lj}]_0|\mathrm{BCS}\rangle_D = \frac{\sqrt{2j+1}}{2}\chi_{\epsilon lj}, \tag{2.4}$$

are given in terms of BCS amplitudes as

$$\chi_{\epsilon lj} \equiv u^P_{\epsilon lj}v^D_{\epsilon lj}\prod_{k\neq(\epsilon lj)}\left(u^P_k u^D_k + v^P_k v^D_k\right). \tag{2.5}$$

The two-proton formation amplitude, according to Eq. (2.1), is given by

$$\begin{aligned} X_{\epsilon lj}[a^\dagger_{\epsilon lj}a^\dagger_{\epsilon lj}] &\to \Psi_{\epsilon lj}(\mathbf{r_1},\mathbf{s_1},\mathbf{r_2},\mathbf{s_2}) \\ &= X_{\epsilon lj}\mathcal{A}\{\psi_{\epsilon lj}(\mathbf{r_1},\mathbf{s_1})\otimes\psi_{\epsilon lj}(\mathbf{r_2},\mathbf{s_2})\}_0 \\ &= \sqrt{2}X_{\epsilon lj}[\psi_{\epsilon lj}(\mathbf{r_1},\mathbf{s_1})\otimes\psi_{\epsilon lj}(\mathbf{r_2},\mathbf{s_2})]_0. \end{aligned} \quad (2.6)$$

The recoupling from the j-j (spin-spin) to the L-S (spin-orbit) scheme gives a superposition between singlet and triplet terms. Because the initial wave function corresponds to the paired two-proton state only the singlet component is relevant. This can be written as

$$\begin{aligned} \Psi^{(0)}_{\epsilon lj}(\mathbf{r_1},\mathbf{r_2}) &= \sqrt{2}X_{\epsilon lj}\left\langle (ll)0,\left(\frac{1}{2}\frac{1}{2}\right)0;0\middle|\left(l\frac{1}{2}\right)j,\left(l\frac{1}{2}\right)j;0\right\rangle \\ &\quad\times[\phi_{\epsilon lj}(\mathbf{r_1})\otimes\phi_{\epsilon lj}(\mathbf{r_2})]_0 \\ &= \sqrt{2}X_{\epsilon lj}\left\langle (ll)0,\left(\frac{1}{2}\frac{1}{2}\right)0;0\middle|\left(l\frac{1}{2}\right)j,\left(l\frac{1}{2}\right)j;0\right\rangle \\ &\quad\times\frac{f_{\epsilon lj}(r_1)f_{\epsilon lj}(r_2)}{r_1r_2}\mathcal{Y}_l(\hat{r}_1,\hat{r}_2) \\ &\equiv \frac{\mathcal{F}_{\epsilon lj}(r_1,r_2)}{r_1r_2}\mathcal{Y}_l(\hat{r}_1,\hat{r}_2), \end{aligned} \quad (2.7)$$

where we defined the two-proton azimuthal harmonics:

$$\begin{aligned} \mathcal{Y}_l(\hat{r}_1,\hat{r}_2) &\equiv [i^lY_l(\hat{r}_1)\otimes i^lY_l(\hat{r}_2)]_0 \\ &= \frac{\sqrt{2l+1}}{4\pi}P_l(\cos\theta)\equiv\mathcal{Y}_l(\cos\theta). \end{aligned} \quad (2.8)$$

Thus, the two-proton dynamics can be described in terms of three coordinates, r_1, r_2, and θ, as in Fig. 1.

The next step is the description of the two-proton emission process. The motion of the two protons beyond the nuclear surface is described by the Schrödinger equation

$$H\psi(\mathbf{r_1},\mathbf{r_2}) = E\psi(\mathbf{r_1},\mathbf{r_2}), \quad (2.9)$$

with outgoing boundary conditions. We suppose that the emitted protons have equal energies, due to the fact that they initially occupy paired states with the same sp energy $\epsilon = E/2$ in Eq. (2.7).

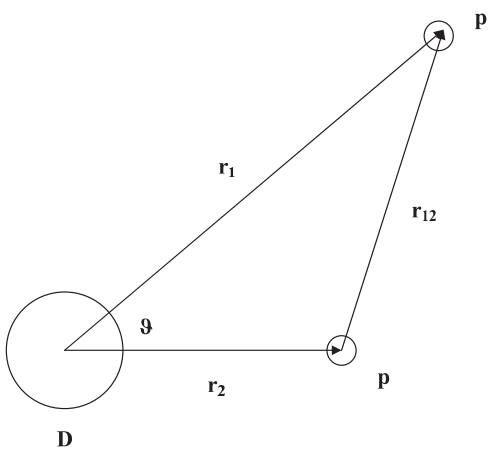

FIG. 1. The geometry of the two-proton emission.

The Hamiltonian in the laboratory system of coordinates is similar to that describing two electrons in a ^{4}He atom [14], i.e.,

$$\begin{aligned} H = &-\frac{\hbar^2}{2\mu r_1}\frac{\partial^2}{\partial r_1^2}r_1 - \frac{\hbar^2}{2\mu r_2}\frac{\partial^2}{\partial r_2^2}r_2 + \frac{\hbar^2}{2\mu}\left(\frac{1}{r_1^2}+\frac{1}{r_2^2}\right)\hat{L}^2 \\ &+ V(r_1)+V(r_2)+v(r_{12}), \end{aligned} \quad (2.10)$$

where $\mu = m_pM_D/(m_p+M_D)$ is the proton reduced mass, $\hat{L}^2$ denotes the standard angular momentum operator squared and the modulus of the relative radius is given by

$$r_{12} = |\mathbf{r}_1-\mathbf{r}_2| = \sqrt{r_1^2+r_2^2-2r_1r_2\cos\theta}. \quad (2.11)$$

The proton-daughter potential is

$$V(r_k) = V_N(r_k)+V_C(Z_De^2,R_D,r_k), \quad k=1,2, \quad (2.12)$$

where $V_N(r_k)$ denotes the nuclear mean field, which we take as a Woods-Saxon potential including the spin-orbit term. The Coulomb potential $V_C(Z_De^2,R_D,r_k)$ corresponds to a homogeneous sphere with charge Z_De, i.e.,

$$\begin{aligned} V_C(Z_De^2,R_D,r_k) = &\frac{Z_De^2}{2R_D}\left(3-\frac{r_k^2}{R_D^2}\right)\Theta(R_D-r_k) \\ &+\frac{Z_De^2}{r_k}\Theta(r_k-R_D), \end{aligned} \quad (2.13)$$

where $R_D = 1.2A_D^{1/3}$ is the daughter radius. We take for the proton-proton interaction a Gaussian form. Therefore the total proton-proton interaction is

$$v(r_{12}) = -v_0e^{-(r_{12}/r_0)^2}+V_C(e^2,r_0,r_{12}). \quad (2.14)$$

where v_0 and r_0 are parameters suggested by scattering nucleon-nucleon experiments, as we see below.

The two-proton wave function can be expanded in terms of the two-proton azimuthal harmonics (2.8) in a fashion similar to that of the monopole pairing wave function (2.7), i.e.,

$$\psi(\mathbf{r_1},\mathbf{r_2}) = \sum_l\frac{g_l(r_1,r_2)}{r_1r_2}\mathcal{Y}_l(\cos\theta), \quad (2.15)$$

and the resulting system of coupled radial equations becomes

$$\begin{aligned} \Big[&-\frac{\hbar^2}{2\mu}\frac{\partial^2}{\partial r_1^2}-\frac{\hbar^2}{2\mu}\frac{\partial^2}{\partial r_2^2}+\frac{\hbar^2l(l+1)}{2\mu}\left(\frac{1}{r_1^2}+\frac{1}{r_2^2}\right) \\ &+V(r_1)+V(r_2)-E\Big]g_l+\sum_{l'}v_{ll'}g_{l'}=0, \end{aligned} \quad (2.16)$$

where the proton-proton matrix elements are given by

$$v_{ll'} = \frac{\hat{l}\hat{l}'}{2}\int_{-1}^{1}v(r_{12})P_l(\cos\theta)P_{l'}(\cos\theta)d\cos\theta. \quad (2.17)$$

Because the proton-daughter potential depends upon lj, in the notation below it has to be understood that $l\to(l,j)$.

To properly satisfy the asymptotic boundary conditions, it is more conveninent to use polar coordinates:

$$\begin{aligned} &r_1 = r\cos\varphi, \quad r_2 = r\sin\varphi, \\ &r\in[0,\infty), \quad \varphi\in\left[0,\frac{\pi}{2}\right]. \end{aligned} \quad (2.18)$$

One can thus describe the two-proton dynamics in terms of one radius, $r = \sqrt{r_1^2 + r_2^2}$, and two angles, φ and θ. This procedure is different than the one in the hyperspherical formalism [3], but the main idea is the same, namely, to obtain a coupled system of equations for the radial components of the wave function with boundary conditions compatible with the emission process. Introducing the function

$$g_l(r,\varphi) = \frac{\overline{g}_l(r,\varphi)}{\sqrt{r}}, \tag{2.19}$$

the system of radial equations contains only second-order derivatives,

$$\left(\frac{\partial^2}{\partial r^2} + \frac{\partial^2}{r^2\partial\varphi^2}\right)\overline{g}_l(r,\varphi) = \frac{2\mu}{\hbar^2}\left[V_l(r,\varphi) - E\right]\overline{g}_l(r,\varphi) + \frac{2\mu}{\hbar^2}\sum_{l'} v_{ll'}(r,\varphi)\overline{g}_{l'}(r,\varphi), \tag{2.20}$$

where

$$V_l(r,\varphi) = \frac{\hbar^2}{2\mu}\left[l(l+1)\left(\frac{1}{r_1^2}+\frac{1}{r_2^2}\right) - \frac{1}{4r^2}\right] + V(r_1) + V(r_2) = \frac{\hbar^2}{2\mu r^2}\left[\frac{4l(l+1)}{\sin^2 2\varphi} - \frac{1}{4}\right] + V(r\cos\varphi) + V(r\sin\varphi) \tag{2.21}$$

is a symmetric function with respect to the exchange of the variables (r_1, r_2) or $(\varphi, \frac{\pi}{2} - \varphi)$. Because the pairing interaction acting upon the two protons induces their clustering [12], as we show below, we expect that the most important contribution is given by the configuration where proton radii are equal to each other, i.e., $r_1 = r_2 = r/\sqrt{2}$, which implies that $\varphi = \pi/4$. Therefore the protons depart from the parent nucleus symmetrically with respect to the angle θ. The case $\varphi \neq \pi/4$ describes a sequential two-proton emission. Thus, "the degree of sequentiality" is described by the difference $\varphi - \pi/4$. Notice that the two extreme cases with $\varphi = 0$ and $\pi/2$ correspond to one-proton decay.

The system of Eqs. (2.20) can be solved by expanding the solution in terms of products between radial and angular functions [15], i.e.,

$$\overline{g}_l(r,\varphi) = \sum_k \mathcal{R}_{lk}(r)\mathcal{Z}_{lk}(r,\varphi), \tag{2.22}$$

where the angular components are eigenstates of the eigenvalue problem given by

$$\left[-\frac{\partial^2}{r^2\partial\varphi^2} + \frac{2\mu}{\hbar^2}V_l(r)\right]\mathcal{Z}_{lk}(r,\varphi) = \lambda_{lk}(r)\mathcal{Z}_{lk}(r,\varphi), \qquad \mathcal{Z}_{lk}(r,0) = \mathcal{Z}_{lk}\left(r,\frac{\pi}{2}\right) = 0. \tag{2.23}$$

In the following we simplify the problem by integrating the system (2.20) for a given angle φ. The system of radial equations becomes

$$\frac{\partial^2\overline{g}_l(r,\varphi)}{\partial r^2} = \frac{2\mu}{\hbar^2}[V_l(r,\varphi) - E]\overline{g}_l(r,\varphi) + \frac{2\mu}{\hbar^2}\sum_{l'} v_{ll'}(r,\varphi)\overline{g}_{l'}(r,\varphi), \tag{2.24}$$

Because the nuclear part of the daughter-proton potential practically vanishes for $r_1, r_2 > R_D$ one obtains a simple expression for $V_l(r)$, namely,

$$V_l(r) \approx \frac{\hbar^2}{2\mu r^2}\left[\frac{4l(l+1)}{\sin^2 2\varphi} - \frac{1}{4}\right] + \frac{Z_D e^2}{r}\left(\frac{1}{\sin\varphi} + \frac{1}{\cos\varphi}\right). \tag{2.25}$$

We have thus reduced the initial entangled dynamics of the system into a rather simple two-body problem.

To check the validity of this approximation we compared the numerical solution $g_l(r,\varphi)$ in the absence of the interproton potential ($v_{ll'} = 0$) with the exact solution, given by the product of Coulomb-Hankel functions $H_l^{(+)}$ for each l, i.e.,

$$g_l^{(\text{exact})}(r,\varphi) = H_l^{(+)}(r\cos\varphi)H_l^{(+)}(r\sin\varphi). \tag{2.26}$$

We obtained $1 \leqslant [\log_{10} g_l / \log_{10} g_l^{(\text{exact})}] \leqslant 1.1$.

To solve the system (2.24) it is convenient to introduce the fundamental matrix of independent solutions [13]. It turns out that the matrix elements of the proton-proton interaction (2.17) decrease as the polar radius r increases. This feature is due to the strong cutoff property of the exponential factor $\exp[-(r/r_0)^2(1-\cos\theta)]$ in Eq. (2.14) at large distances. Therefore the fundamental matrix of solutions at large distances has practically a diagonal form and each element is given by the product of one-proton outgoing Coulomb waves, i.e.,

$$\mathcal{H}_{lk}^{(+)}(r,\varphi) \underset{r\to\infty}{\longrightarrow} \delta_{lk} H_l^{(+)}(r\cos\varphi)H_l^{(+)}(r\sin\varphi), \tag{2.27}$$

where k labels that element. The general solution is given by the superposition of different columns

$$g_l(r,\varphi) = \sum_k N_k \mathcal{H}_{lk}^{(+)}(r,\varphi) \underset{r\to\infty}{\longrightarrow} N_l H_l^{(+)}(r\cos\varphi)H_l^{(+)}(r\sin\varphi). \tag{2.28}$$

The coefficients defining the scattering amplitudes [13], are determined by matching the general solution with the internal radial wave function (2.7). One thus gets

$$g_{l'}(r,\varphi) = \sum_k N_k \mathcal{H}_{l'k}^{(+)}(r,\varphi) = \mathcal{F}_{\epsilon lj}(r\cos\varphi, r\sin\varphi)\delta_{ll'}, \tag{2.29}$$

where ϵlj are the sp quantum numbers of the initial state. In the absence of the proton-proton interaction one obtains only one nonvanishing scattering amplitude corresponding to the quantum numbers of the initial paired state:

$$N_l = \sqrt{2}X_{\epsilon lj}\left\langle (ll)0, \left(\frac{1}{2}\frac{1}{2}\right)0; 0 \middle| \left(l\frac{1}{2}\right)j, \left(l\frac{1}{2}\right)j; 0\right\rangle M_{\epsilon lj}^2. \tag{2.30}$$

By applying the Schrödinger equation with complex energy $E - i\Gamma/2$ one obtains in a standard fashion the total decay width by integrating over θ [13]:

$$\Gamma(\varphi) = (\sin\varphi + \cos\varphi)\hbar v \sum_l |N_l|^2. \tag{2.31}$$

The total width is given by

$$\Gamma = \frac{2}{\pi}\int_0^{\pi/2} \Gamma(\varphi) d\varphi. \tag{2.32}$$

III. NUMERICAL APPLICATION

We investigate the two-proton emitters ^{45}Fe and ^{48}Ni. The first nucleus is superfluid, while the second one is in a normal proton phase. The experimental values of the energies and half-lives are $E = 1.14 \pm 0.04$ MeV and $T = 4.7(+3.4, -1.4)$ ms for ^{45}Fe [16] and $E = 1.35 \pm 0.02$ MeV and $T = 2.1(+2.1, -0.7)$ ms for ^{48}Ni [17]. For the central nuclear field we use a standard Woods-Saxon potential with universal parametrization [18]. The strength of the potential was adjusted to reproduce the available experimental two-proton emission energy $E = 2\epsilon$.

The nuclear structure properties are described by the wave function amplitudes $X_{\epsilon lj}$ in Eq. (2.4). The u and v occupation amplitudes are evaluated as usually, i.e., by solving the BCS equations for the parent and daughter nuclei, respectively. To solve the internal problem in a self-consistent way with respect to the external two-proton dynamics, we evaluated the pairing matrix elements entering BCS equations by using a similar proton-proton interaction given by Eq. (2.14). Details of the estimation of the pairing interaction matrix elements, which depend upon relative coordinates, in terms of absolute coordinates can be found in Ref. [19].

In Ref. [20] the coherent length of the pairing interaction, estimated by using the Gogny force, has a much larger value inside the nucleus than in the external region. Figure 5 of this Ref. [20], corresponding to Ni isotopes, predicts a mean coherence length of about 6 fm in the internal region, decreasing as one approaches the nuclear surface and reaching the value of 2 fm just outside the nucleus. Actually one expects that the size of any cluster increases when going from outside to inside the nucleus because inside the Pauli blocking hinders nucleons to cluster together and, therefore, the cluster loses binding and becomes larger.

In the evaluation of the proton-proton interaction (2.14) we adopted the value $r_0^{(\mathrm{int})} = 6$ fm for the size parameter. We found that larger values of $r_0^{(\mathrm{int})}$ have a smoothing effect on the pairing gap as a function of the sp level.

We estimated the quantity $\chi_{\epsilon lj}$, Eq. (2.5), corresponding to the two-proton emission from ^{45}Fe as a function of the sp state number k. In Fig. 2 we averaged this quantity over neighboring states to smooth out local oscillations. For comparison the uv product in the parent nucleus (dashed line) and the same quantity in the daughter nucleus (dot-dashed line) are also shown. The decaying state corresponds to the Fermi level $k = 7$, with $\epsilon = 0.57$ MeV, $l = 3$, and $j = 7/2$. For the normal phase, like in ^{48}Ni, we use in the parent nucleus a sharp distribution around the Fermi surface

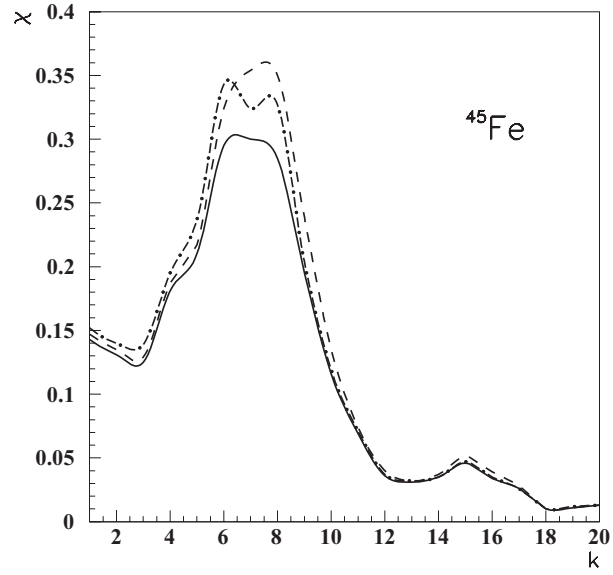

FIG. 2. The function $\chi_{\epsilon lj}$ [Eq. (2.5)], which is proportional to the formation amplitude (2.4), corresponding to the two-proton emission from ^{45}Fe as a function of the sp state number (solid line). The dashed line is the uv product in the parent nucleus and the dot-dashed line is the same product in the daughter nucleus. The Fermi level is at $k = 7$. The parameters of the pairing interaction in Eq. (2.14) are $v_0 = 35$ MeV and $r_0 = 2$ fm.

and compute the two-proton wave function corresponding to Eq. (2.7).

As mentioned above, near the nuclear surface the pairing interaction induces a clustering of the two protons. One thus expects that at that position the corresponding wave function acquires its maximum value. This is indeed the case, as shown in Fig. 3(a), where the wave function is plotted as a function of the radial coordinate r. A similar clustering feature can be seen on the φ coordinate. In Fig. 3(b) we plotted the dependence of the wave function upon the angle φ for the radius $r = 6$ fm, corresponding to the wave function maximal value. One sees that the two-proton distribution reaches its maximal value at $\varphi = 45^\circ$, corresponding to the symmetric configuration $r_1 = r_2$.

We performed the matching of the internal wave function with the outgoing solution in the region beyond the maximal value of the internal wave function. But it is important to stress that the continuity of the wave function's first derivative requires that the computed half-life $T = \hbar ln2/\Gamma$ should not depend on the matching radius in this region. How well the half-life thus obtained satisfies this criterion is a measure of the quality of the calculation.

We first estimated the half-life by using the decoupled ansatz $[v(r_{12}) = 0]$ of the scattering amplitude given by Eq. (2.30). The value of T thus obtained overestimates the corresponding experimental value by 4 orders of magnitude. This shows that the proton-proton interaction (2.14) plays a crucial role in the two-proton dynamics. We adopted for the radial parameter r_0 of the nuclear (Gaussian) potential in $v(r_{12})$ [Eq. (2.14)] the value $r_0 = 2$ fm.

We investigated the influence of the proton-proton interaction upon the decay process by changing the potential

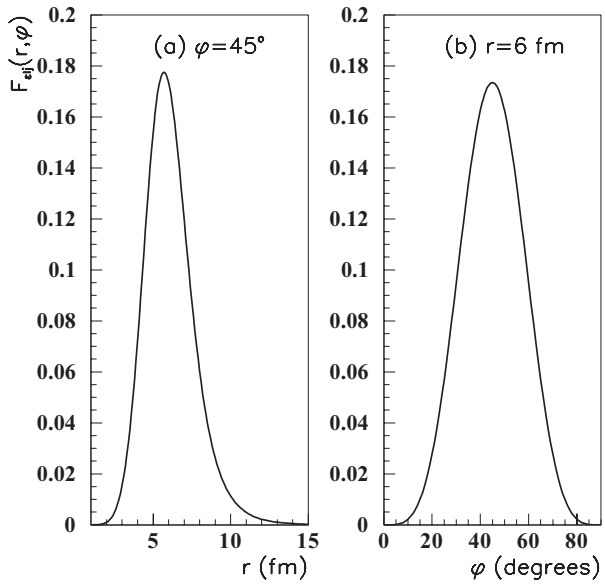

FIG. 3. (a) Two-proton radial wave function in ^{45}Fe, given by Eq. (2.7), as a function of the coordinate r for $\varphi = 45^\circ$. The parameters of the proton-proton interaction in Eq. (2.14) are $v_0 =$ 35 MeV and $r_0 = 2$ fm. (b) Same as in panel (a) but as a function of the angle φ corresponding to the maximal value of the wave function at $r = 6$ fm.

strength v_0. Concerning the strength parameter in the internal region, we kept a constant ratio $v_0/v_0^{(\mathrm{int})} = 4$, reproducing the experimental pairing gap for the realistic value of the proton-proton strength v_0. The proton pairing gap increases as a function of the interaction strength v_0, as is shown in Fig. 4 for ^{45}Fe.

The specific feature of the three-body scattering problem is that the relative distance between the emitted protons can be small ($\varphi \approx 45^\circ$) for any radius between their center of mass

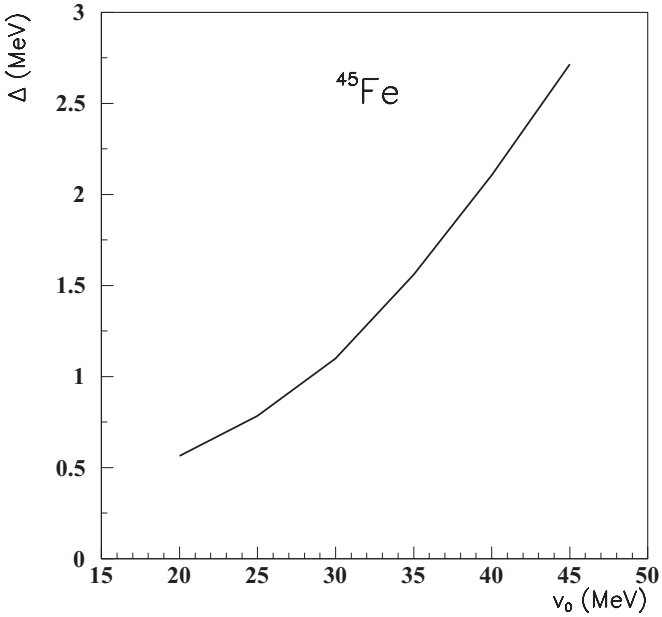

FIG. 4. Proton pairing gap versus proton-proton strength v_0 in ^{45}Fe.

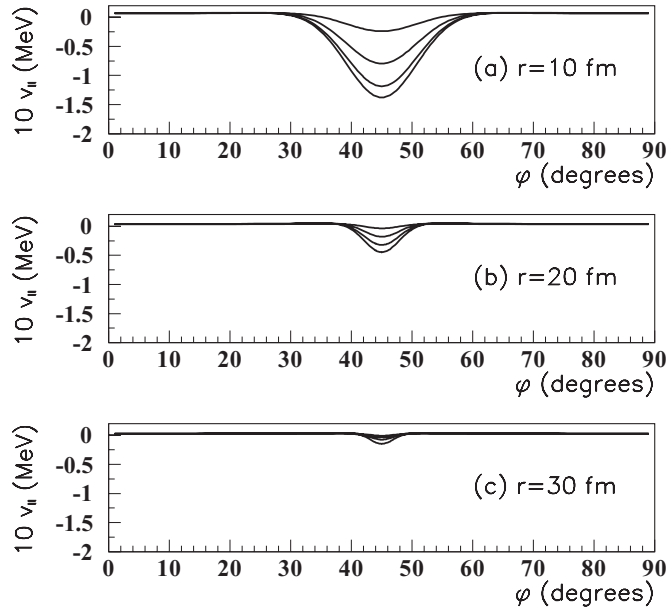

FIG. 5. Diagonal matrix elements (2.17) versus angular variable φ for $r = 10$ fm (a), $r = 20$ fm (b), and $r = 30$ fm (c). The proton-proton interaction in Eq. (2.14) is defined by $v_0 = 35$ MeV and $r_0 =$ 2 fm.

and the daughter nucleus. This implies that the solution at large distances of $r = \sqrt{r_1^2 + r_2^2}$ never decouples. But it has to be stressed that at $r = 50$ fm the interaction matrix elements are 2 orders of magnitude smaller with respect to their values on the nuclear surface. This is illustrated in Fig. 5, where we have plotted the diagonal matrix elements given by Eq. (2.17) as a function of the angular variable φ for $r = 10$ fm (a), $r = 20$ fm (b), and $r = 30$ fm (c). Notice that the interaction matrix elements are concentrated in a rather narrow interval between 40° and 50° around the symmetric configuration and they rapidly decrease with distance. Thus, the decoupled ansatz (2.27) can be considered as a rather good approach at large distances for any angular variable φ.

We computed the partial angular decay width, given by Eq. (2.31). In Fig. 6 we give the result corresponding to the matching radius $r = 7$ fm and the strength parameter $v_0 =$ 35 MeV in ^{45}Fe. One sees that the width is concentrated in a very narrow interval, i.e., $\varphi = 45^\circ \pm 2^\circ$, thus showing that the symmetric configuration $r_1 = r_2 = r/\sqrt{2}$ has the dominant role.

In Fig. 7 we plotted the half-life as a function of the matching radius r, lying beyond the geometrical nuclear radius, for several values of v_0. Notice that the corresponding sp radii are given by Eq. (2.18). The first feature to be noticed is the weak dependence of the half-life upon the matching radius around the nuclear surface. This confirms that the derivative of the internal and external wave functions are approximately equal; i.e., the so-called "plateau condition" is fulfilled [13], thus endorsing the validity of our calculation.

The strong influence of the proton-proton interaction strength v_0 upon the half-life is also noteworthy. This is due to the coupling of the initial channel, with $l = 3$, to the monopole channel, with $l = 0$, giving the largest partial decay

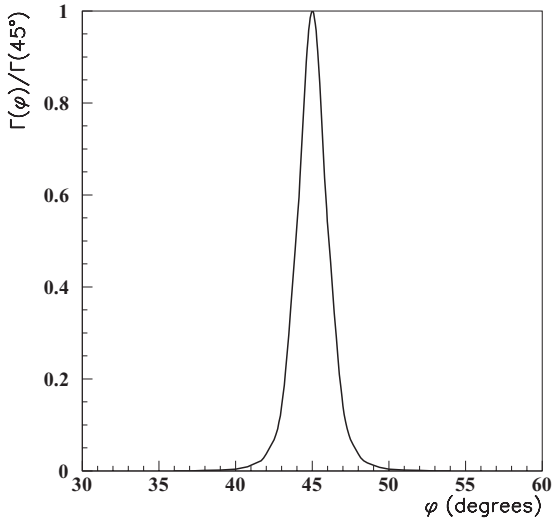

FIG. 6. The ratio of the angular-dependent width given by Eq. (2.31) and its value at $\varphi = 45^\circ$ versus the angle φ for $v_0 = 35$ MeV and $r_0 = 2$ fm.

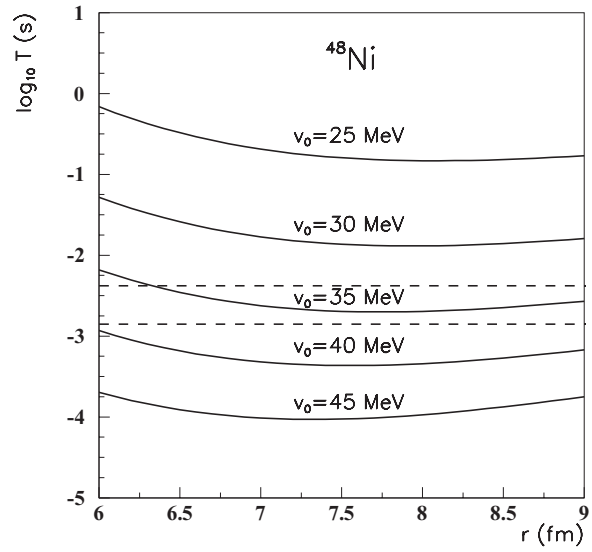

FIG. 8. Same as in Fig. 7, but for ^{48}Ni.

width (and therefore the lowest partial half-life). Figure 7 shows that this coupling becomes larger by increasing the proton-proton coupling strength. The experimental interval for the half-life (between dashed lines) corresponds to a proton-proton strength of $v_0 \in [30, 35]$ MeV, i.e., close to its realistic value $v_0 = 35$ MeV [5]. The corresponding value of the pairing gap in Fig. 4 is also close to the realistic value, which is $\Delta \approx 1.3$ MeV for Fe isotopes in this region.

We performed similar calculations for ^{48}Ni. This nucleus is magic in protons and therefore they are in a normal phase. This leads to a smaller pairing density and decay width. Therefore the half-life is slightly larger for the same coupling strength v_0. This is confirmed by Fig. 8, where the experimental value corresponds to a larger coupling strength of $v_0 \in [33, 37]$ MeV.

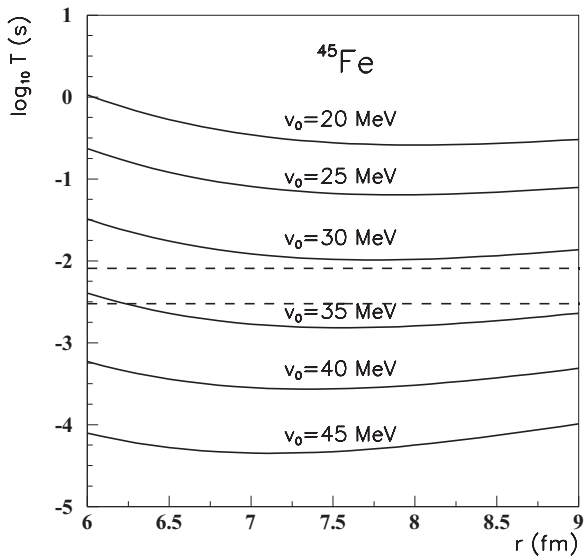

FIG. 7. Theoretical two-proton half-life for ^{45}Fe, versus the matching proton radius for various proton-proton interaction strengths v_0 in Eq. (2.14) (solid lines). The dashed lines indicate the upper and lower experimental limits.

IV. CONCLUSIONS

In conclusion we have described in this paper the two-proton emission process from spherical nuclei by using a simple formalism. We considered that the two particles are emitted from a correlated pairing state. The proton-proton potential was chosen to have a Gaussian form besides the Coulomb interaction. We treated the BCS equations and the external dynamics in a self-consistent way, by using similar proton-proton interactions.

It would be incorrect to make an analogy with α decay and consider the decaying system as a simple diproton. The decay proceeds neither through a diproton particle nor as an uncorrelated two-proton channel but rather as a configuration in between these two extremes.

We have shown that the partial decay width is strongly peaked around the symmetric configuration $r_1 = r_2$, in the interval $\varphi = 45^\circ \pm 2^\circ$. An important feature is that the formalism predicts a strong dependence of the half-life upon the proton-proton coupling strength. We thus conclude that two-proton emission is a powerful tool not only to uncover the nuclear degrees of freedom determining the nuclear dynamics, especially the pairing mode, but also to investigate the evolution of the proton-proton potential from the nuclear medium to regions well outside the nucleus.

ACKNOWLEDGMENTS

This work has been supported by Grant No. PN-II-ID-PCE-2011-3-0092 of the Romanian Ministry of Education and Research and by the Swedish National Research Council. Discussions with Professor I. Mukha and Professor L. Ixaru are greatfully acknowledged.

[1] V. I. Goldansky, Nucl. Phys. **19**, 482 (1960).
[2] P. Swan, Rev. Mod. Phys. **37**, 336 (1965).
[3] L. V. Grigorenko, R. C. Johnson, I. G. Mukha, I. J. Thompson, and M. V. Zhukov, Phys. Rev. C **64**, 054002 (2001).
[4] L. V. Grigorenko and M. V. Zhukov, Phys. Rev. C **68**, 054005 (2003), and references therein.
[5] L. V. Grigorenko, I. A. Egorova, M. V. Zhukov, R. J. Charity, and K. Miernik, Phys. Rev. C **82**, 014615 (2010).
[6] R. A. Kryger *et al*., Phys. Rev. Lett. **74**, 860 (1995).
[7] B. A. Brown and F. C. Barker, Phys. Rev. C **67**, 041304(R) (2003), and references therein.
[8] J. Rotureau, J. Okolowicz, and M. Ploszajczak, Phys. Rev. Lett. **95**, 042503 (2005).
[9] J. Rotureau, J. Okolowicz, and M. Ploszajczak, Nucl. Phys. A **767**, 13 (2006).
[10] D. S. Delion, R. J. Liotta, and R. Wyss, Phys. Rep. **424**, 113 (2006).
[11] D. S. Delion, Phys. Rev. C **80**, 024310 (2009).
[12] F. A. Janouch and R. J. Liotta, Phys. Rev. C **27**, 896 (1983).
[13] D. S. Delion, *Theory of Particle and Cluster Emission* (Springer-Verlag, Berlin, New York, 2010).
[14] C. W. David, The Hamiltonian and Schrödinger Equation for Helium's Electrons (Hylleraas), preprint 6-5-2006, University of Connecticut, DigitalCommons@UConn, 2006.
[15] L. Ixaru, Comput. Phys. Commun. **181**, 1738 (2010).
[16] J. Giovinazzo *et al*., Phys. Rev. Lett. **89**, 102501 (2002).
[17] C. Dossat *et al*., Phys. Rev. C **72**, 054315 (2005).
[18] J. Dudek, W. Nazarewicz, and T. Werner, Nucl. Phys. A **341**, 253 (1980).
[19] D. S. Delion, M. Baldo, and U. Lombardo, Nucl. Phys. A **593**, 151 (1995).
[20] N. Pillet, N. Sandulescu, and P. Schuck, Phys. Rev. C **76**, 024310 (2007).